

# Lawrence Berkeley National Laboratory

## Lawrence Berkeley National Laboratory

### Title

Temporal development of the plasma composition of Zr and Cr metal plasma streams in a N<sub>2</sub> environment

### Permalink

<https://escholarship.org/uc/item/55d5w4mx>

### Authors

Rosen, Johanna  
Anders, Andre  
Hultman, Lars  
[et al.](#)

### Publication Date

2003-01-31

# **Temporal development of the plasma composition of Zr and Cr metal plasma streams in a N<sub>2</sub> environment**

Johanna Rosén

Department of Physics, Linköping University, Linköping SE-58183, Sweden

André Anders

Lawrence Berkeley National Laboratory, Berkeley, California 94720, USA

Lars Hultman

Department of Physics, Linköping University, Linköping SE-58183, Sweden

Jochen M. Schneider

Materials Chemistry, RWTH-Aachen, D-52056 Aachen, Germany

## **ABSTRACT**

We describe the temporal development of the plasma composition in a pulsed plasma stream generated by cathodic arc. Cathodes of Zr and Cr were operated at various nitrogen pressures. The time resolved plasma composition for the cathode materials was analysed with time-of-flight charge-to-mass spectrometry, and was found to be a strong function of the nitrogen pressure. Large plasma composition gradients were detected within the first 60  $\mu\text{s}$  of the pulse, the nitrogen ion concentration increasing with increasing pressure. The results are explained by the formation and erosion of a compound layer formed at the cathode surface in the presence of a reactive gas. The average charge state was also found to be affected by the reactive gas pressure as well

as by the time after ignition. The charge states were highest in the beginning of the pulse at low nitrogen pressure, decreasing to a steady-state value at higher pressure. These results are of importance for reactive plasma processing and for controlling of the evolution of thin film composition and microstructure.

## I. INTRODUCTION

In a cathodic arc discharge, the plasma production at the cathode surface facilitates the current transport between the electrodes. The plasma originates from micrometer-sized cathode spots of very high current, power and plasma density [1], resulting in a highly ionized plasma, which can be used for thin film synthesis, ion implantation and ion injection into accelerators.

The cathode spot exhibits an unstationary behavior and depends strongly on the surface chemistry. Extensive studies have been performed on its appearance and behaviour, on contaminated surfaces (type 1 spots) and on clean surfaces (type 2 spots) [2,3]. Contaminated surfaces originate from either residual gas present in the chamber or intentionally introduced gas. Since the cathode surface is the feed-stock material for the plasma, it is straightforward to understand that such contamination will affect the resulting plasma chemistry and therefore also the charge state of the various species. The individual ion charge states are of importance in plasma processing. This is because the kinetic energy gain across the potential difference between plasma and substrate is proportional to the charge state, and it is well known that the kinetic energy, and therefore also the charge states, affect the microstructure evolution and hence the film properties [4].

The vacuum arc plasma composition and the average ion charge states of most conductive elements have been measured by Brown and Godechot [5] and theoretically simulated by Anders [6]. Similar experimental investigations have also

been performed in the presence of a reactive gas. For example, Oks *et al.* [7] reported reduced ion charge states of Al as the oxygen pressure increased, and Spädtke *et al.* [8] showed the influence of nitrogen pressure on Mo, Fe and Ti ion currents. The investigators have obtained similar results showing that both the concentration as well as the average charge state decreases as the pressure is increased. These data, however, were collected in the steady-state regime of the arc pulse with a delay of  $\geq 100 \mu\text{s}$  with respect to arc ignition [5,7], or correspond to the ion current resulting from integration of the total arc pulse [8]. To see the effect of a compound layer formed in the presence of a reactive gas, a time-resolved analysis is needed.

Very limited data are available describing the temporal development of a cathodic arc. Anders and Jüttner [9] observed a temporal change of the plasma composition in measurements of the ion energy. Schneider *et al.* [10] reported the temporal development of a pulsed aluminum plasma stream at various oxygen pressures. These data suggest that the plasma chemistry and the average Al charge state are strong functions of both oxygen pressure and time into the pulse. The results were explained by the formation and erosion of a compound layer at the cathode surface.

In this study we have analysed the temporal evolution of the plasma chemistry for Zr and Cr plasma streams in the presence of nitrogen. We find that there is a concentration gradient of nitrogen ions in the beginning of the arc pulse, which is strongly dependent on cathode material and pressure. The findings are relevant since the temporal development of the plasma chemistry and average charge states may be important for the evolution of film composition and structure, respectively.

## II. EXPERIMENTS

The analysis of the plasma composition was carried out using a time-of-flight (TOF) charge-to-mass spectrometer at Lawrence Berkeley National Laboratory, described in detail in Ref. 11, and shown schematically in Fig. 1. An ion beam is formed by extraction of ions from the plasma source, the distance between the source and the extraction system being  $\sim 0.1$  m. A set of annular electrostatic TOF gates is used to select a 200 ns sample of the beam, which is allowed to drift to a magnetically suppressed Faraday cup located 1.03 m from the TOF gate. From the measured ion current-time dependence, as exemplified in Fig. 2 for a Zr cathode, the plasma composition can be calculated, since the flight of the different ionic species in the beam depends on their charge-to-mass ratio.

Arc pulses with a duration of  $\sim 300$   $\mu\text{s}$  were generated from cathodes with a diameter of 6.25 mm, at a pulse repetition rate of 0.8 Hz, and at an arc current of 200 A. The extractor voltage forming the ion beam was set to 30 kV. To obtain temporal resolution, the 200 ns sample selected by the TOF gate was scanned through the arc pulse. Time zero was chosen to be the time when the first ions from the arc pulse reached the extraction system, approximately 10  $\mu\text{s}$  after arc ignition, thus corresponding to the beginning of the beam pulse. Using an adjustable delay generator for the TOF, the pulse was scanned in time steps of 5  $\mu\text{s}$  (within the first 30  $\mu\text{s}$ ), 10  $\mu\text{s}$  (up to 100  $\mu\text{s}$ ) and finally in steps of 25 and 50  $\mu\text{s}$ . The data were collected at a base pressure of  $8 \times 10^{-7}$  Torr, and after introducing nitrogen up to four different levels, the highest corresponding to a partial pressure of  $1 \times 10^{-4}$  Torr.

### III. EXPERIMENTAL RESULTS

For the measurements described, we collected data in the form of averages, where  $\sim 25$  arc pulses resulted in a stabilized average. We here present in detail the most relevant results for Zr, and discuss briefly the results of Cr at the end of this section.

In Fig. 3, the average charge state of Zr is shown as a function of time and nitrogen pressure, calculated from the measured individual Zr ion charge state distributions. At lower pressures the average charge state is strongly dependent on time, the largest changes being within the first 100  $\mu\text{s}$ . The extreme case is found at a pressure of  $5 \times 10^{-6}$  Torr, where the average charge state decreases from 3.1 in the beginning of the pulse to 2.4 at the end of the pulse. As the pressure is increased the time dependence becomes less pronounced and the average charge state gradually decreases. At  $1 \times 10^{-4}$  Torr a steady state is reached at a charge state of 1.9.

The plasma contained Zr, N and O ions. Small traces of H were also observed, but a meaningful quantification was not possible due to a signal close to noise level. Figures 4, 5, and 6 show the Zr, N and O plasma composition, respectively, in at.% of the total plasma composition. All compositions are given versus time into pulse and nitrogen partial pressure. Only the first 100  $\mu\text{s}$  are shown since the time after that represents the steady-state regime of ion formation where no significant changes are detected (measured up to 250  $\mu\text{s}$ ). All three graphs show a strong temporal dependence of the plasma composition, extending over the entire pressure range measured and concentrated within the first 60  $\mu\text{s}$  of the pulse. At low pressures the plasma consisted of Zr, N and O, both N and O most clearly seen within the first 30

$\mu\text{s}$ , with values of up to 30-40% and 10% respectively. The relative amount of oxygen never exceeded 10 %, and as the pressure increased, the traces of oxygen decreased in amount as well as in how far into the pulse the traces are seen. This is in contrast to nitrogen, which increased up to 60% at 25  $\mu\text{s}$  and at a pressure of  $5 \times 10^{-5}$  Torr. The high nitrogen content also extended further into the pulse; for higher pressures the nitrogen content was 20% up to 50  $\mu\text{s}$ , before it decreased to approximately 5%.

A pressure and temporal dependence of both the plasma chemistry and the average charge state were found also for Cr, though not as pronounced. Cr plasma showed a maximum concentration of nitrogen ions of  $\sim 20\%$  measured at  $1 \times 10^{-4}$  Torr nitrogen gas pressure, which decreased gradually during the first 30-40  $\mu\text{s}$  down to a nitrogen ion fraction of  $\sim 5\%$ , which was the steady state value. When the pressure was decreased, the time dependence was less pronounced, and below  $1 \times 10^{-5}$  Torr steady state was reached. The average ion charge state of Cr showed qualitatively the same development as for Zr, with a maximum of 2.6 in the beginning of the pulse at lower pressure and a minimum of 1.6 in the steady state regime at the highest pressure, as seen in Fig. 7.

Another effect caused by an increasing nitrogen pressure was the reduction of the measured total ion current signal for both metals studied, which is consistent with previous findings [8].



#### IV. DISCUSSION

The effect of a reactive gas on plasma production in a cathodic arc process can be subdivided into: (a) the interaction at the cathode surface and its immediate vicinity, and (b) the interaction in the plasma expansion volume. In the absence of a magnetic field (a) is dominating the plasma composition evolution. [12]

Since the pressure in the spot exceeds atmospheric pressure by orders of magnitude, the presence of a gas affects the spot processes indirectly. Depending on gas and cathode material, chemical reactions may occur at the cathode surface, forming a compound surface layer, also referred to as a poisoned layer. The surface temperature associated with plasma production in cathodic arc spots may facilitate chemical diffusion, affecting the thickness of the compound layer.

Kühn *et al.* [13] investigated the surface chemistry of Zr, Cr, and Ti cathodes operated in a nitrogen atmosphere. Using Rutherford Backscattering Spectrometry (RBS) measurements on samples cut from worn cathodes (operated in nitrogen gas), information on average concentration and depth distribution of nitrogen was obtained, as listed in Table I. For Zr, the results were 16 at.% in a nitride layer of average thickness  $\leq 0.1 \mu\text{m}$ . Ref. 13 therefore indicates that a nitrided layer is formed.

A compound surface layer affects both the spot ignition mechanism and the plasma production process, as compared to a clean surface. One distinguishes between spots of type 1 (occurring on contaminated surfaces) and of type 2 (on clean surfaces). On a

clean surface the ignition of a spot may be caused by explosion of metallic microtips, the basic electron emission being thermofield emission [9]. The type 2 spot then moves a distance not exceeding its crater radius, leading to chains of overlapping craters [2]. On a contaminated surface the dielectric layers cause additional electron emission mechanisms, which favor the formation of new spots. As a result, type 1 spots on contaminated surfaces tend to show random movement over larger distances than type 2 spots on clean surfaces [2,9,14,15].

Detailed studies of the structure of cathode spots show clear differences between type 1 and type 2 [2,9]. With clean surfaces in UHV there are usually just a few spots producing craters with a radius of 5-10  $\mu\text{m}$ . Introducing a background gas, spot splitting is favored as the pressure increases, resulting in several simultaneously existing active spots leaving craters with a diameter of less than 1  $\mu\text{m}$ . This small crater radius implies a short spot lifetime and therefore less erosion. This is evident in a comparison between pictures of erosion tracks on clean and contaminated surfaces [2]. The spot velocity is also affected by contaminants. Ellrodt *et al.* [14] reported the influence of cathode material and ambient gas on the motion and velocity of the cathode spots. They found that in general the spot arrangement and motion were similar on various metals as the surface was contaminated, and the velocity of the spots increased. Differences were found between contaminated layers of high conductivity and insulating layers, the former showing only slight increase of the spot velocity as the pressure increased.

From this point forward, we will use the general discussion above together with further selected properties of the cathode materials to suggest an explanation for the

phenomena observed. The main (first) part of the discussion will concern the results of the Zr cathode, but after that a comparison between Zr and Cr will also be made, followed by a short discussion concerning the importance of these findings.

The temporal development of the plasma composition versus nitrogen partial pressure reported here for Zr can be explained in terms of the cathode surface chemistry and associated implications for the cathode spot motion: At base pressure, the cathode surface reacts chemically with both nitrogen and oxygen, stemming from residual gas [10, 12]. As the arc is ignited, the cathode spot runs over the surface and erodes this layer, resulting in a time dependent plasma chemistry evolution in the beginning of the pulse. The existence of type 1 spots depends on surface state and volume of nitrated/oxidized material. After approximately 60  $\mu\text{s}$ , the arc burns on bulk material and a steady state regime is reached. As the nitrogen pressure increases, the oxygen concentration gradually decreases while the nitrogen concentration increases. According to Ref. 13 a nitrated layer is formed at the Zr cathode surface. Therefore, spots of type 1 will prevail in the beginning of the arc pulse, resulting in smaller spots with shallow craters. Type 1 spots run faster over the nitrated surface, as compared to the motion on a clean surface at base pressure. Since the arc spots runs preferentially over the nitrated area, the compound layer will be eroded first, followed by a transition to type 2 spots, which erode the clean Zr surface.

As the nitrogen partial pressure is increased, the nitrogen concentration-time distribution increases both in amplitude and width, as shown in Fig. 5. This can be understood in terms of chemical diffusion occurring at the cathode surface, which may result in the formation of a thicker nitrated layer and/or a layer changing in

composition towards higher nitrogen content as the pressure increases. One crucial parameter affecting the formation of this compound layer is the pulse repetition rate [17], the time available between the pulses for the cleaned surface to regain its previous nitrated state. Another parameter of great importance is the size of the cathode surface, since it affects the ability to form a new nitrated layer *during* the pulse, in areas already cleaned by the cathode spots.

For discussing the evolution of the compound layer chemistry and hence the plasma composition, we need to consider both energetics and kinetics. Gibb's free energy of formation  $\Delta G$ , the enthalpy of formation  $\Delta H$ , and possible phase changes for the nitrides taken from literature, are given in Table II.  $\Delta G$  and  $\Delta H$  are temperature dependent (in Table II given at room temperature), and so is the diffusion constant  $D_N$  of nitrogen in the cathode material. The temperature distribution of the cathode surface is not well defined. The temperature field extends from the temperature of the cooling water in the bulk of the cathode, to  $\sim 43\ 000$  K at the Zr cathode spot (the plasma temperature), as seen in Table I. Very steep temperature gradients into the cathode both with respect to geometry and time can be expected. The magnitude of the temperatures involved suggests that the activation energies for the diffusion processes can be overcome. The nitrogen diffusion constant measurements reported in the literature are characterized by large scattering, and for Zr (in the solid state)  $D_N$  is limited to  $1 \times 10^{-9}$  mm<sup>2</sup>/s (extrapolated data) [22]. Generally, as the temperature approaches the melting temperature of the material, the curve of  $D_N$  might exhibit a small upward curvature, as compared to the extrapolated line, followed by an increase in the diffusion constant of several orders of magnitude in the liquid at the melting temperature [23,24].

Based on the above considerations with respect to energetics and kinetics we suggest that the cathode surface chemistry is affected by chemical diffusion processes. This is consistent with the strong temporal development of the concentration gradients observed in Figures 4-6. From that we propose that the resulting plasma chemistry is mainly a result of the chemistry at or close to the cathode surface.

As the partial pressure is increased, the probability for collisions of the metal ions with the gas is increased. The effect of this interaction is evident from the reduced total ion current signal measured, as mentioned above. This behavior can be understood in terms of a collision-induced change from a plasma beam (mean free path larger than source-TOF distance) towards a more isotropic plasma expansion (mean free path less than source-TOF distance. Another possible consequence of scattering is, apart from a change in direction of the plasma expansion, also that charge exchange collisions may occur [25]. Effects thereof are seen in the average charge state of the metal ions, seen in Fig. 3. At lower pressure the average charge state of Zr shows a temporal development that is strongest during the first 50  $\mu\text{s}$  of the arc pulse. The higher charge states observed there is a result of more energy being invested in the plasma at the beginning of the pulse [26]. As the plasma expands further into the chamber it can do so without suffering from many collisions with gas molecules, with the result that we measure a plasma traveling more or less undisturbed from the cathode surface. As the pressure increases above  $1 \times 10^{-5}$  Torr, the time dependence of the plasma chemistry is less pronounced. The reason is the increased probability of collisions in the plasma due to the presence of numerous gas molecules. Energetically favorable reactions may occur, with the result that the

concentration of ions with lower charge increases at the expense of ions with higher charge. Changes in the average charge state of Zr during the pulse, resulting from the process at the cathode surface, are therefore not detected. A steady state regime is reached, that is characterized by a lower average charge state.

The discussion above explaining the time- and pressure dependence of the plasma originating from a Zr cathode is qualitatively consistent with the data measured for Cr plasma streams. The investigation in Ref. 13 included also Cr as a cathode material, where the nitrogen concentration was found to be under the detection limit. Our investigation suggests the existence of a compound layer on Cr, but only at higher nitrogen pressures. Both metals show a similar pressure dependent effect; erosion of a nitrated layer at the cathode surface causing a temporal dependence of the plasma chemistry. A Zr cathode results in the highest nitrogen content in the plasma, while Cr has not as high levels.

For pressures below  $1 \times 10^{-5}$  Torr, Zr shows a strong temporal dependence with up to 40 % of nitrogen in the beginning of the pulse. In the same pressure range Cr shows hardly any temporal dependence at all with the steady state value of 5 %. If the cathode surface chemistry could be based on energetics, Zr would be the most nitrated material, but the result of Cr would be more pronounced, see Gibb's free energy of formation in Table II. A measurable effect of nitridation for Cr would then be expected. As the pressure increases, nitrogen concentration gradients are found also for Cr, though the detected levels for Zr are 2-3 times higher. Our measurements together with the RBS-measurements in Ref. 13 therefore suggest that the nitridation of the surface is based on *both* energetics and kinetics.

A direct comparison of the diffusion constants of the materials is not straight forward, due to insufficient experimental data (though the extrapolated limitation for  $D_N$  in Zr and Cr is approximately the same) as well as the unknown temperature distribution of the cathode surfaces. The calculations of the plasma temperature in the cathode spot (Table I) may indicate that the surface temperature peak of the Zr cathode is somewhat higher, probably resulting in higher diffusion of nitrogen in Zr as compared to Cr. What should also be considered is the difference in how sensitive the materials are to temperature changes and nitride formation. Zr and Cr have approximately the same melting temperature, but behave differently when forming nitrides. The nitrides of Cr are more sensitive to temperature as compared to Zr, since they decompose at temperatures lower than the melting point of the pure metal. Zr on the other hand forms a nitride that melts more than 1000 K above the melting temperature of pure Zr. Therefore, in order to discuss the chemical diffusion more thoroughly, one need to know both the temperature distribution and the diffusion mechanisms present, both in the pure cathode materials and the nitrides formed.

These results for Zr and Cr in nitrogen are qualitatively consistent with the explanation given in Ref. 10 for Al in oxygen. Therefore, a temporal development of the plasma composition, caused by the formation and erosion of a compound layer, seems to be a general effect of a reactive gas in a pulsed cathodic arc process. To what extent it can be expected depends on the material and its reactivity, and also on parameters like arc current, pressure, geometry of the cathode and pulse repetition rate, as mentioned above. A similar temporal dependence may also be expected in plasma processes other than cathodic arc, especially other pulsed processes.

A pressure and temporal dependence of the plasma composition are of importance in reactive plasma processing and thin film synthesis: An expression for the kinetic energy of an ion is given by  $E_i = E_0 + Qe\Delta U$ , where  $E_0$  is the initial kinetic energy of the ion gained at the cathode spot,  $Q$  is the charge state of the ion, and  $\Delta U$  is the potential difference in the sheath in front of the substrate.  $E_0$  has been measured by Bilek *et al.* for a Ti arc discharge in a nitrogen environment [27], and has in general been found to be pressure dependent [27,28]. Further, through  $\Delta U$ , the ion energy can be controlled by selecting the substrate bias. The resulting energy is known to affect the microstructure evolution (and therefore also the material properties) of the resulting film, through its effects on for example defect formation, nucleation density and adatom mobility [4]. The expression shows the importance of the plasma composition, both concerning what species are present (affecting the compositional evolution of the film) and their charge states (affecting the ion energy). These findings may pertain to plasma producing processes, in particular pulsed processes, where there is a cathode surface in a reactive environment.

## V. CONCLUSIONS

We present evidence for a strong temporal dependence of the plasma composition in a pulsed cathodic arc (Zr, Cr) in a reactive gas environment ( $N_2$ ). A large non-metal fraction is observed in the plasma at the beginning of the pulse, and as the pressure increases, this fraction increases both in amplitude as well as in time after arc ignition. These findings can be understood by the formation of a nitrated cathode surface layer, a result of both energetics and kinetics, promoting the existence of type 1 cathode



spots. These spots run preferentially over the nitrated areas, cleaning the cathode until a surface of metallic bulk material is exposed, leading to a steady state of the concentration of non-metal ion species in the plasma. Furthermore, the average metal ion charge state is found to be a function of both time into the pulse and gas pressure. The pressure dependence of the plasma chemistry is caused by both varying nitridation of the cathode surface, and varying interaction between the expanding metal plasma and the surrounding gas. These results are of importance for reactive plasma processing, through an increased understanding of the evolution of the thin film composition (through plasma composition) and microstructure of the film (through the charge states and therefore also the ion energy).

## **ACKNOWLEDGEMENTS**

This work was supported by the Swedish Foundation for Strategic Research (SSF) Materials Research Program on Low Temperature Thin Film Synthesis and by the U.S. Department of Energy under Contract No. DE-AC03-76SF00098 at Lawrence Berkeley National Laboratory. One of the authors (J.M.S.) acknowledges sponsorship of the Alexander von Humboldt Foundation, the Federal Ministry of Education and Research, and the Program for Investment in the Future.

## References:

- [1] A. Anders, S. Anders, B. Jüttner, W. Bötticher, H. Lück, and G. Schröder, IEEE Trans. Plasma Sci. **20**, 466 (1992)
- [2] G. A. Mesyats, *Cathode Phenomena in a Vacuum Discharge: The Breakdown, the Spark and the Arc* (Nauka, Moscow, 2000)
- [3] B. Jüttner, J. Phys. D: Appl. Phys. **34**, R103 (2001)
- [4] J. E. Greene, S. A. Barnett, J.-E. Sundgren, and A. Rocket, *Ion Beam Assisted Thin Film Growth*, edited by K. Itoh (Elsevier, Amsterdam, 1989), Chap. 5.
- [5] I. G. Brown, Rev. Sci. Instrum. **65**, 3061 (1994)
- [6] A. Anders, Phys. Rev. E, **55**, 969 (1997)
- [7] E. Oks and G. Yushkov, Proc. XVIIth International Symposium on Discharges and Electrical Insulation in Vacuum, Berkeley, 584 (1996)
- [8] P. Spädtke, H. Emig, and B. H. Wolf, Rev. Sci. Instrum. **65**, 3113 (1994)
- [9] S. Anders and B. Jüttner, IEEE Trans. Plasma Sci. **19**, 705 (1991)
- [10] J. M. Schneider, A. Anders, I. Brown. B. Hjörvarsson, and L. Hultman, Appl. Phys. Lett. **75**, 612 (1999)
- [11] I. G. Brown, J. E. Galvin, R. A. MacGill, and R. T. Wright, Rev. Sci. Instrum. **58**, 1589 (1987)
- [12] J. M. Schneider, A. Anders, B. Hjörvarsson, and L. Hultman, Appl. Phys. Lett. **76**, 1531 (2000)
- [13] M. Kühn and F. Richter, Surf. Coat. Technol. **89**, 16 (1997)
- [14] M. Ellrodt and M. Kühn, Contrib. Plasma Phys. **36**, 687 (1996)
- [15] G. E. Kim, J.-L. Meunier, and F. Ajersch, IEEE Trans. Plasma Sci. **23**, 1001 (1995)

- [16] *Thermodynamic Properties of Inorganic Materials: Pure Substances*, Landolt-Börnstein IV vol.19 A1, (Springer, Berlin, 1999)
- [17] G. Yushkov and A. Anders, *IEEE Trans. Plasma Sci.* **26**, 220 (1998)
- [18] I. Barin, and O. Knacke, *Thermochemical Properties of Inorganic Substances* (Springer, Berlin, 1973)
- [19] *Handbook of Chemistry and Physics, 72<sup>nd</sup> edition*, (CRC Press, Boston, 1991)
- [20] L. E. Tooth, *Transition Metal Carbides and Nitrides* (Academic Press, New York and London, 1971)
- [21] *Phase Equilibria, Crystallographic and Thermodynamic Data of Binary Alloys*, Landolt-Börnstein IV vol.5D, (Springer, Berlin, 1999)
- [22] *Diffusion in Solid Materials and Alloys*, Landolt-Börnstein III vol.26, (Springer, Berlin, 1990)
- [23] R. E. Reed-Hill, *Physical Metallurgy Principles, 2nd ed.* (PWS Publishers, Boston, 1973)
- [24] R. W. Cahn and P. Haasen (editors) *Physical Metallurgy, Third edition* (North Holland Physics Publishing, Amsterdam, 1983)
- [25] B. Chapman, *Glow Discharge Processes* (John Wiley & Sons, New York, 1980)
- [26] A. Anders and G. Yushkov, *J. Appl. Phys.* **91**, 4824 (2002)
- [27] M. M. M. Bilek, P. J. Martin, and D. R. McKenzie, *J. Appl. Phys.* **83**, 2965 (1998)
- [28] M. M. M. Bilek, M. Chhowalla, and W. I. Milne, *Appl. Phys. Lett.* **71**, 1777 (1997)

**Figure captions:**

Figure 1: Simplified schematic of the high vacuum ion source with a time-of-flight (TOF) charge-to-mass spectrometer.

Figure 2: Ion current versus TOF, measured at 40  $\mu\text{s}$  into the pulse and at a nitrogen partial pressure of  $5 \times 10^{-5}$  Torr.

Figure 3: Average ion charge state of Zr vs nitrogen pressure (Torr) and time into arc pulse ( $\mu\text{s}$ ).

Figure 4: Zr ion concentration in the plasma (%) vs nitrogen pressure (Torr) and time into arc pulse ( $\mu\text{s}$ ).

Figure 5: N ion concentration in the plasma (%) vs nitrogen pressure (Torr) and time into arc pulse ( $\mu\text{s}$ ).

Figure 6: O ion concentration in the plasma (%) vs nitrogen pressure (Torr) and time into arc pulse ( $\mu\text{s}$ ).

Figure 7: Average ion charge state of Cr vs nitrogen pressure (Torr) and time into arc pulse ( $\mu\text{s}$ ).

## Tables

Table I: Cathode materials and selected properties.

Table II: Stable nitrides formed from the cathode materials investigated. M=melting,  
D=decomposition.

Figure 1, Rosén et al, JAP

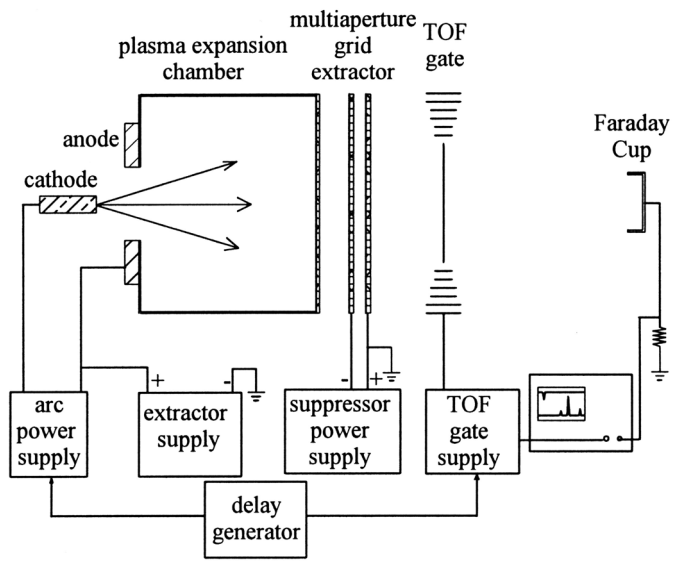


Figure 2, Rosén et al, JAP

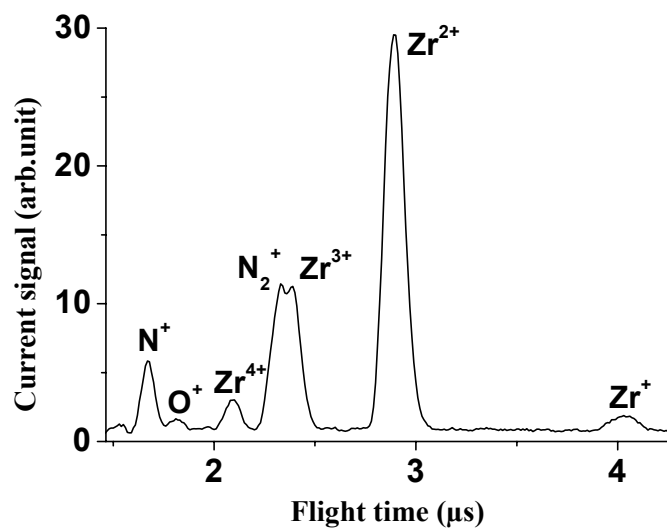


Figure 3, Rosén et al, JAP

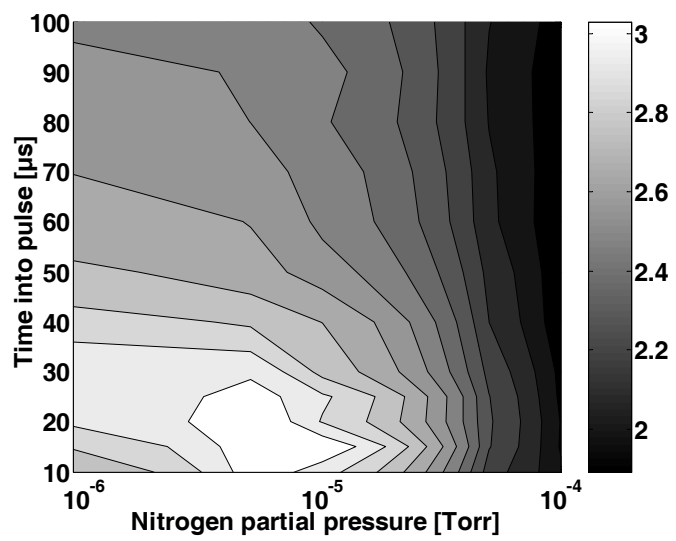




Figure 4, Rosén et al, JAP

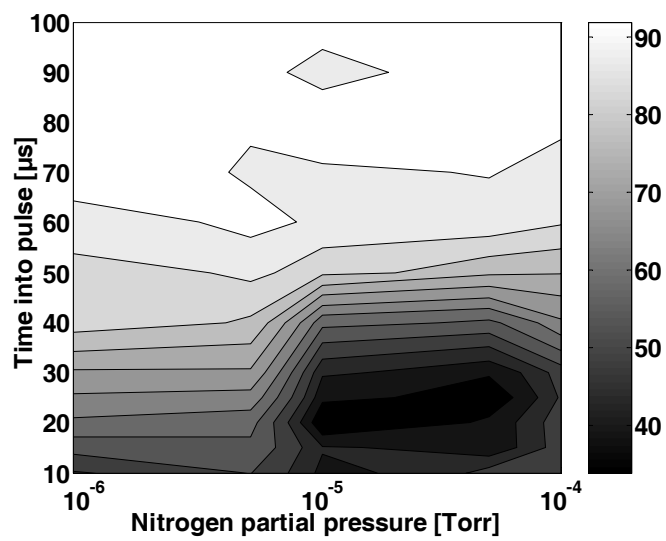


Figure 5, Rosén et al, JAP

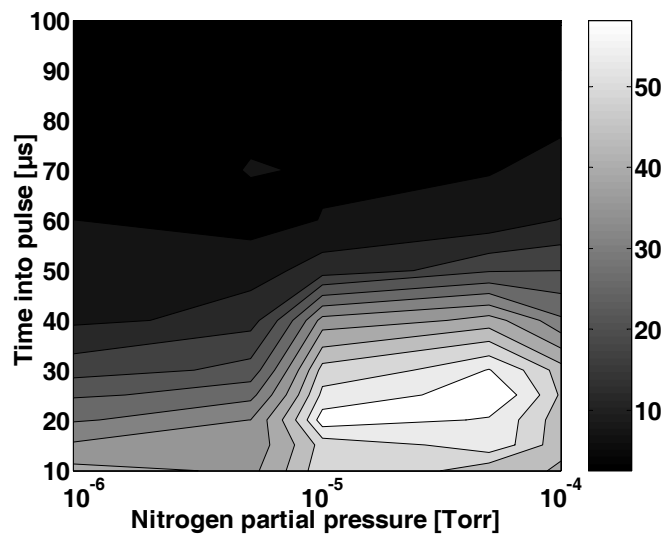


Figure 6, Rosén et al, JAP

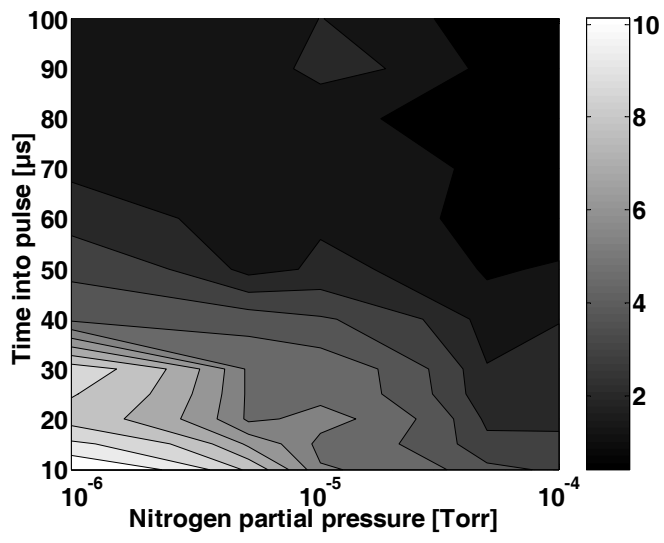


Figure 7, Rosén et al, JAP

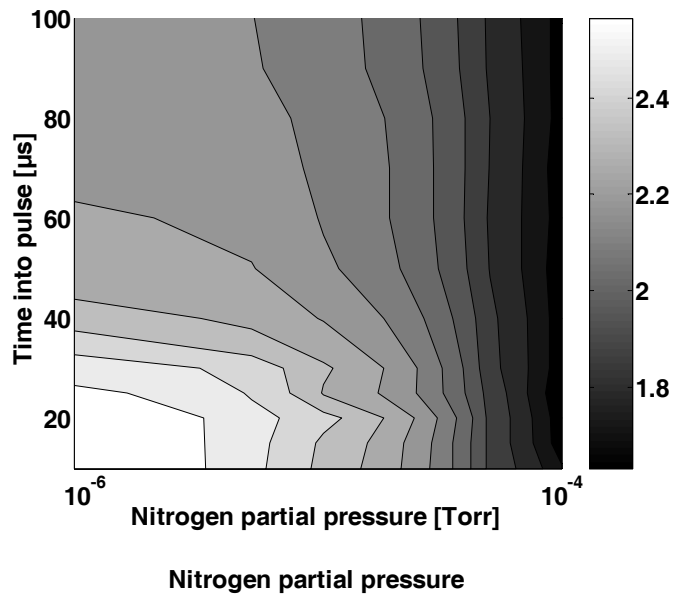


Table I, Rosén et al, JAP

<b>Metal</b>	<b>T<sub>melt</sub> (K)</b> [16]	<b>T<sub>plasma</sub> at c. spot (eV)</b> [6]	<b>RBS-measurement of cathode (at.% N)</b> [13]
<b>Zr</b>	2128	3.7 (~43000 K)	16 in depth $\leq 0.1\mu\text{m}$
<b>Cr</b>	2180	3.4 (~39000 K)	Under detect. limit.

Table II, Rosén et al, JAP

<b>Nitride</b>	<b><math>\Delta G</math> (kJ/mol) [18]</b>	<b><math>\Delta H</math> (kJ/mol) [19]</b>	<b>Phase changes</b>
<b>ZrN</b>	-377	-365	M: 3250 K [20]
<b>Cr<sub>2</sub>N</b>	-150	-128	D: ~1900-2000 K [21]
<b>CrN</b>	-133	-125	D: ~1970 K [19]